Accepted Manuscript

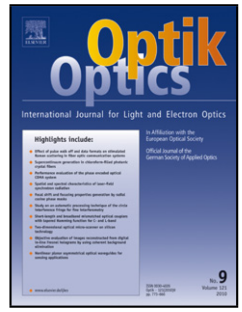


Title: A Back Propagation neural network based optimizing model of space-based large mirror structure

Authors: Zhongshan Wang, Jingxu Zhang, Jixin Wang, Xin He, Liangliang Fu, Fuxiang Tian, Xiaofeng Liu, Yuchen Zhao

PII: S0030-4026(18)31474-8
DOI: https://doi.org/10.1016/j.ijleo.2018.09.161
Reference: IJLEO 61600

To appear in:

Received date: 31-7-2018
Accepted date: 28-9-2018

Please cite this article as: Wang Z, Zhang J, Wang J, He X, Fu L, Tian F, Liu X, Zhao Y, A Back Propagation neural network based optimizing model of space-based large mirror structure, *Optik* (2018), https://doi.org/10.1016/j.ijleo.2018.09.161

# A Back Propagation neural network based optimizing model of space-based large mirror structure

WANG Zhongshan[a,b,*], ZHANG Jingxu[a], WANG Jixin[c], HE Xin[a], FU Liangliang[a], TIAN Fuxiang[a], LIU Xiaofeng[a], ZHAO Yuchen[a]

*([a]Changchun Institute of Optics, Fine Mechanics and Physics., Chinese Academy of Sciences, Changchun 130033, China*
*[b]University of Chinese Academy of Sciences, Beijing 100049, China*
*[c]School of Mechanical Science and Engineering, Jilin University, Changchun 130033, China*

*[*]Corresponding author:* WANG Zhongshan, *Changchun Institute of Optics, Fine Mechanics and Physics., Chinese Academy of Sciences, No.3888 Dongnanhu Road, Changchun 130033, China, Tel:+86043186708593, Email:hitwzs@126.com)*

**Abstract:**

Weight, dynamic characteristic and the surface shape error of space-based large mirror depend on mirror structure parameters which include monolithic central thickness, rib thickness, face sheet thickness etc. In order to obtain the nonlinear mapping relation between target characteristics and design variables for mirror structure optimization, we present a prediction model based on Back Propagation (BP) neural network. Training samples and test samples of neural network were obtained by taking advantage of orthogonal test design and finite element analysis software Patran/Nastran. We built a prediction model by adjusting transfer function, the number of neurons in hidden layer and training algorithm to meet requirements. Extrapolation performance of this prediction network was validated by test samples. Then, we can find optimal combination for mirror structure parameters under certain conditions by the prediction network. The results indicate that the prediction value of this network agree well with the numerical simulation results, relative error are less than or equal to 7.09%. The neural network can predict mirror characteristics accurately enough, so that it can optimize mirror structure parameters. This method can also be applied to other structure optimization.

**Keyword:** large mirror; BP neural network; finite element analysis; orthogonal test design

## 1. Introduction

With today's drive toward extremely large aperture systems, development of large aperture mirror was a urgent need for long-focus, large-aperture space camera[1-2]. With the aperture becoming larger, the weight of mirror will become larger accordingly. So that its surface figure accuracy was hard to maintain[3-4]. The surface figure accuracy will influence image quality of space camera, so it is key technology to maintain surface figure accuracy of large aperture mirror for space camera[5-6]. The target characteristic of mirror including weight, dynamic characteristic and the surface shape error under the effect of gravity depend on structure parameters including monolithic central thickness, face sheet thickness, rib thickness etc. How to obtain the optimal target characteristic of mirror with multi-parameter inputs deserve detailed study.

Neural networks are good at nonlinear functions fitting, so that it can deal with complex nonlinear issues[7-9]. In fact, there is proof that a fairly simple neural network can fit any practical function. Furthermore, neural network has no limit with input node[10-11], thus it is fit for solving optimization with multi-parameter inputs. BP neural network is multilayer feedforward network that train weights with nonlinear differentiable function. BP neural network is most widely used in the field of pattern recognition, function approximation, data compression etc[12-14].

This issue studies the multi-parameter optimization of large space-based mirror structure based on BP neural network. We build finite element analysis model based on mirror geometric model. Training sample and test sample of neural network were obtained by taking advantage of orthogonal test design and the finite element analysis software Patran/Nastran, so that we obtain target value of their corresponding inputs. We build BP neural network model using Matlab toolbox, and verify extrapolation performance of network. Finally, we can obtain the optimal parameters combination by means of the BP network model with certain condition.

## 2. Optimize parameters of mirror structure

After material selection, the target characteristics of mirror including weight, dynamic characteristic and the surface shape error under the effect of gravity are directly influenced by mirror structure. A round mirror with diameter 2.8m, as primary mirror of a space camera was studied in this issue. Its finite element model is detailed in Fig.1. Open lighten structure was selected on the back of mirror, and lightweight hole were triangle which had isotropy and well stability. Although the surface figure error can be reduced suitably small by gravity compensation, the mirror itself must have enough stiffness and stability[15]. According to finite element analysis results, main structure parameters that influence surface figure error and dynamic stiffness include monolithic central thickness, face sheet thickness, rib thickness and outermost wall thickness. They decide the weight of mirror together.

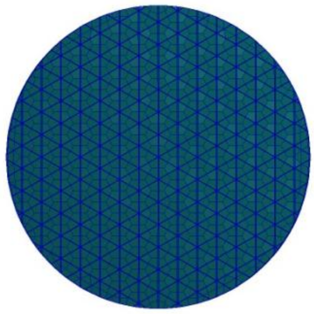

Figure 1 Finite element model of mirror

## 3. BP neural network non-linear mapping model

### 3.1 Principle of BP neural network

BP neural network is error back propagation neural network. It is usually composed of input layer, hidden layer and output layer. Neurons between back layer and front layer are completely connected with weights, that is, any neuron in the front layer is connected with each and every neuron in the back layer, and neurons in the same layer are not connected. Back propagation algorithm includes input signal forward-propagation and error signal back propagation. In the forward-propagation, samples are from input layer, go through each hidden layer and output layer. If actual output has deviation with target output, output error will be back propagated from output layer to input layer layer-by-layer. The output error will be distributed to all neurons in each layer to form element error for each neuron. each neuron weight will be tuned based on element error. Through signal forward-propagation and error back propagation, weights of network are tuned gradually until output error is reduced in acceptable range or iterations reach a certain given value.

A two-layer feed-forward network with sigmoid hidden neurons and linear output neurons can fit multi-dimensional mapping problems arbitrarily well, given consistent data and enough neurons in its hidden layer. Structure of multi-layer neural network with one hidden layer is shown in Fig.2.

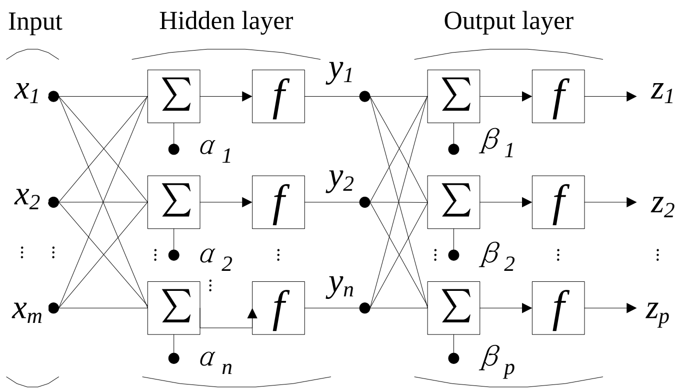

Figure 2 Structure of multi-layer neural network with one hidden layer

The process of input signal forward-propagation is as follows,

suppose input are $x_1,x_2,\ldots,x_i,\ldots,x_m$, output of hidden layer are $y_1,y_2,\cdots,y_j,\cdots,y_n$, output of network are $z_1,z_2,\cdots,z_k,\cdots,z_p$, target output are $Z_1,Z_2,\cdots,Z_k,\cdots,Z_p$, weights from input layer to hidden layer are $v_{ij}$, weights from hidden layer to output layer are $w_{jk}$, bias of hidden layer are $\alpha_j$, bias of output layer are $\beta_k$, among them $i=1,2,\cdots,m$, $j=1,2,\cdots,n$, $k=1,2,\cdots,p$. First of all, weights and bias of all neurons are assigned random smaller value. Through forward-propagation, output of hidden layer and output layer are as follows

$$y_i = f\left(\sum_{i=1}^{m} v_{ij} x_i - \alpha_j\right)$$

$$z_k = f\left(\sum_{j=1}^{n} w_{jk} y_j - \beta_k\right)$$

Among the formula, $f(.)$ is transfer function. Tan-sigmoid transfer function, log-sigmoid and linear transfer function are widely used. Generally speaking, sigmoid function is selected in the output layer in the field of pattern recognition, and linear function is selected in the output layer in the field of nonlinear function approximation. When output is not equal to target output, output error is as follows

$$E = \frac{1}{p}\sum_{k=1}^{p}(Z_k - z_k)^2 \qquad (1)$$

The development of Eq. (1),

$$E = \frac{1}{p}\sum_{k=1}^{p}(Z_k - f(\sum_{j=1}^{n} w_{jk} y_j - \beta_k))^2 =$$
$$\frac{1}{p}\sum_{k=1}^{p}(Z_k - f(\sum_{j=1}^{n} \omega_{jk} f(\sum_{i=1}^{m} v_{ij} x_i - \alpha_j) - \beta_k))^2$$

It is observed that, output error of network is function of weights and bias. The output error can be reduced by tuning weights and bias. Training process will finished after multiple learning iterations till output error meets requirements.

### 3.2 Model of neural network

The input of neural network are monolithic central thickness, face sheet thickness, rib thickness and outermost wall thickness, and the output of neural network are weight of mirror, first order constraint mode and the surface shape error RMS(Root Mean Square) under axial gravity. The neural network that be composed of one hidden layer and one output layer is adopted to build prediction model for mirror structure parameters. As shown in Fig.3, $x_1,x_2,x_3,x_4$ represent monolithic central thickness, face sheet thickness, rib thickness and outermost wall thickness respectively, and $M$, $f_1$,$RMS$ represent weight of mirror, first order constraint mode and the surface shape error RMS under axial gravity respectively.

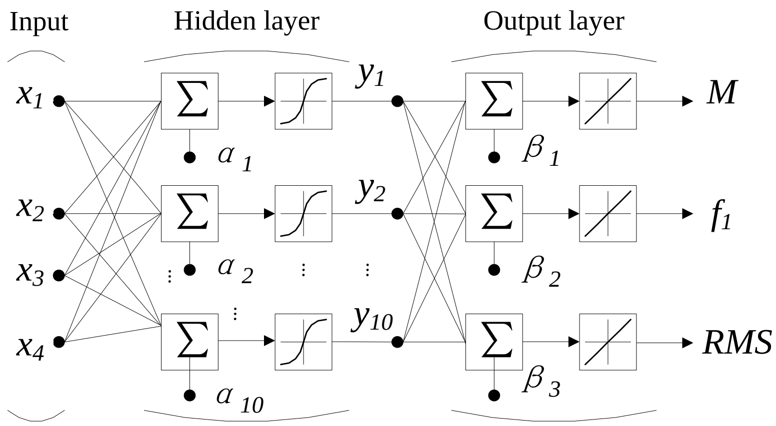


Figure 3 Structure of neural network with one hidden layers and four inputs

In this issue, we take advantage of Matlab toolbox for BP neural network building, training and testing. The network is trained with L-M(Levenberg-Marquardt) back propagation algorithm. Its convergence rate is faster than others when network weights are less. Number of hidden layer neurons deeply influence output error, training time and extrapolation performance of network. It is hard to describe the complex relation contained in sample and study capacity is less when hidden layer neurons are too few. On the contrary, overfitting will be come out when hidden layer neurons is too many. Usually, we select the number of hidden layer neurons with cut-and -try method. Finally, we choose 10 hidden layer neurons to make up a 4-10-3 network.

### 3.3 Training sample

Training sample is foundation base of neural network design. Its scientific rationality will influence the quality of network. In this issue, inputs of network have 4 factors, and each input factor has 6 levels. Test factor and level are shown in Tab.1. If full-scale test are conducted, the test number will reach $6^4$=1296. Obviously, workload is too high to accomplish.

Table 1 Test factor and level

| Level | Factor | | | |
|---|---|---|---|---|
| | $x_1$(mm) | $x_2$(mm) | $x_3$(mm) | $x_4$(mm) |
| 1 | 180 | 4 | 3 | 5 |
| 2 | 190 | 5 | 4 | 6 |
| 3 | 200 | 6 | 5 | 7 |
| 4 | 210 | 7 | 6 | 8 |
| 5 | 220 | 8 | 7 | 9 |
| 6 | 230 | 9 | 8 | 10 |

In order to maintain ergodicity, representativeness and error tolerant, orthogonal test design is adopted in this issue. It arranges and analysis multi-factor test with orthogonal table. The data in orthogonal table are selected from full-scale test which have representativeness. Based on character of orthogonal table, these data in orthogonal table have the character of "uniformity, dispersion, orderliness and comparability". Orthogonal test can reduce test number by a large margin and then it is equivalent to full-scale test. In consideration of test factor and level, we form orthogonal table shown in Tab.2, and acquire training sample for network with FEM software. Training samples are shown in Tab.3 as follow.

Table 2 Orthogonal test design table

| Serial number | Colum | | | |
|---|---|---|---|---|
| | $x_1(mm)$ | $x_2(mm)$ | $x_3(mm)$ | $x_4(mm)$ |
| 1 | 1(180) | 1(4) | 1(3) | 1(5) |
| 2 | 1(180) | 2(5) | 2(4) | 2(6) |
| 3 | 1(180) | 3(6) | 3(5) | 3(7) |
| 4 | 1(180) | 4(7) | 4(6) | 4(8) |
| 5 | 2(190) | 5(8) | 5(7) | 5(9) |
| 6 | 2(190) | 6(9) | 6(8) | 6(10) |
| 7 | 2(190) | 1(4) | 2(4) | 3(7) |
| 8 | 2(190) | 2(5) | 3(5) | 4(8) |
| 9 | 3(200) | 3(6) | 4(6) | 5(9) |
| 10 | 3(200) | 4(7) | 5(7) | 6(10) |
| 11 | 3(200) | 5(8) | 6(8) | 1(5) |
| 12 | 3(200) | 6(9) | 1(3) | 2(6) |
| 13 | 4(210) | 1(4) | 3(5) | 4(8) |
| 14 | 4(210) | 2(5) | 4(6) | 5(9) |
| 15 | 4(210) | 3(6) | 5(7) | 6(10) |
| 16 | 4(210) | 4(7) | 6(8) | 1(5) |
| 17 | 5(220) | 5(8) | 1(3) | 2(6) |
| 18 | 5(220) | 6(9) | 2(4) | 3(7) |
| 19 | 5(220) | 1(4) | 4(6) | 5(9) |
| 20 | 5(220) | 2(5) | 5(7) | 6(10) |
| 21 | 6(230) | 3(6) | 6(8) | 1(5) |
| 22 | 6(230) | 4(7) | 1(3) | 2(6) |
| 23 | 6(230) | 5(8) | 2(4) | 3(7) |
| 24 | 6(230) | 6(9) | 3(5) | 4(8) |

Table 3 Input and output of training samples

| Serial number | Colum | | | | $M(Kg)$ | $f_1(Hz)$ | $RMS(nm)$ |
|---|---|---|---|---|---|---|---|
| | $x_1(mm)$ | $x_2(mm)$ | $x_3(mm)$ | $x_4(mm)$ | | | |
| 1 | 180 | 4 | 3 | 5 | 313.0158 | 132.14 | 842.538 |
| 2 | 180 | 5 | 4 | 6 | 406.4400 | 132.69 | 847.434 |
| 3 | 180 | 6 | 5 | 7 | 499.8642 | 133.03 | 850.544 |
| 4 | 180 | 7 | 6 | 8 | 593.2884 | 133.29 | 852.536 |
| 5 | 190 | 8 | 7 | 9 | 712.1124 | 138.33 | 786.877 |
| 6 | 190 | 9 | 8 | 10 | 809.0848 | 138.51 | 787.568 |
| 7 | 190 | 4 | 4 | 7 | 408.2864 | 136.1 | 783.367 |
| 8 | 190 | 5 | 5 | 8 | 505.2587 | 136.71 | 785.804 |
| 9 | 200 | 6 | 6 | 9 | 624.3641 | 141.68 | 729.767 |

| | | | | | | | |
|---|---|---|---|---|---|---|---|
| 10 | 200 | 7 | 7 | 10 | 724.8846 | 142.03 | 730.614 |
| 11 | 200 | 8 | 8 | 5 | 782.9227 | 144.66 | 766.102 |
| 12 | 200 | 9 | 3 | 6 | 441.0504 | 134.97 | 756.438 |
| 13 | 210 | 4 | 5 | 8 | 522.7205 | 144.12 | 694.175 |
| 14 | 210 | 5 | 6 | 9 | 626.7892 | 144.9 | 692.043 |
| 15 | 210 | 6 | 7 | 10 | 730.8578 | 145.47 | 690.537 |
| 16 | 210 | 7 | 8 | 5 | 790.7556 | 148.53 | 721.148 |
| 17 | 220 | 8 | 3 | 6 | 444.3196 | 144.81 | 635.637 |
| 18 | 220 | 9 | 4 | 7 | 551.9364 | 147.37 | 627.442 |
| 19 | 220 | 4 | 6 | 9 | 629.2142 | 147.11 | 666.292 |
| 20 | 220 | 5 | 7 | 10 | 736.8309 | 148.12 | 660.582 |
| 21 | 230 | 6 | 8 | 5 | 826.1294 | 155.67 | 643.325 |
| 22 | 230 | 7 | 3 | 6 | 436.1003 | 150.06 | 583.582 |
| 23 | 230 | 8 | 4 | 7 | 547.2652 | 152.18 | 580.541 |
| 24 | 230 | 9 | 5 | 8 | 658.4300 | 153.4 | 580.064 |

### 3.4 Validation of extrapolation performance

Extrapolation refers to the performance that network predict some samples other than training sample. Whether the neural network is of practical value depends on its extrapolation performance. In the range of input values, we choose 6 arrays randomly as test samples to test extrapolation performance of neural network. The prediction values of test samples can be acquired from network. Prediction values and numerical simulation results are shown in Tab.4 respectively.

Table 4 Comparison of neural network prediction and numerical simulation

| Serial number | Test samples | | | | *M(Kg)* | | | *f₁(Hz)* | | | *RMS(nm)* | | |
|---|---|---|---|---|---|---|---|---|---|---|---|---|---|
| | $x_1$ (mm) | $x_2$ (mm) | $x_3$ (mm) | $x_4$ (mm) | NN Prediction | FEA | Relative error% | NN Prediction | FEA | Relative error% | NN Prediction | FEA | Relative error% |
| 1 | 180 | 8 | 6 | 6 | 619.79 | 599.96 | 3.31 | 132.75 | 134.11 | 1.01 | 834.48 | 867.25 | 3.78 |
| 2 | 190 | 5.5 | 6 | 7 | 585.46 | 578.78 | 1.15 | 138.13 | 137.81 | 0.23 | 794.99 | 805.53 | 1.31 |
| 3 | 200 | 5.5 | 5 | 7 | 525.68 | 526.62 | 0.18 | 140.83 | 142.25 | 1.42 | 739.47 | 729.01 | 1.43 |
| 4 | 200 | 6 | 6 | 8 | 616.52 | 617.28 | 0.12 | 142.00 | 142.23 | 0.16 | 738.29 | 734.99 | 0.45 |
| 5 | 210 | 5 | 8 | 6 | 756.23 | 758.70 | 0.33 | 151.13 | 145.56 | 3.83 | 693.71 | 746.68 | 7.09 |
| 6 | 210 | 6 | 6 | 5 | 615.11 | 617.05 | 0.31 | 148.63 | 148.28 | 0.24 | 705.90 | 702.78 | 0.44 |

We can see from Tab.4, to predict mirror weight and first order constraint mode with this neural network prediction model, its relative error are less than or equal to 3.83%. It is slightly weak to predict the surface shape error RMS under axial gravity using this model with maximum relative error 7.09%. However, its prediction relative error are less than or equal to 3.78% other than the fifth test sample. Thus it can be seen, this neural network prediction model can describe mapping relation between mirror target characters and mirror structure parameters accurately enough.

The following regression plots in Fig.4 display the network outputs with respect to targets for training, validation, and test sets. For a perfect fit model, the data should fall along a 45 degree line, where the network outputs are equal to the targets. For this problem, the fit is reasonably good for all data sets, with R values in each case of 0.99 or above.

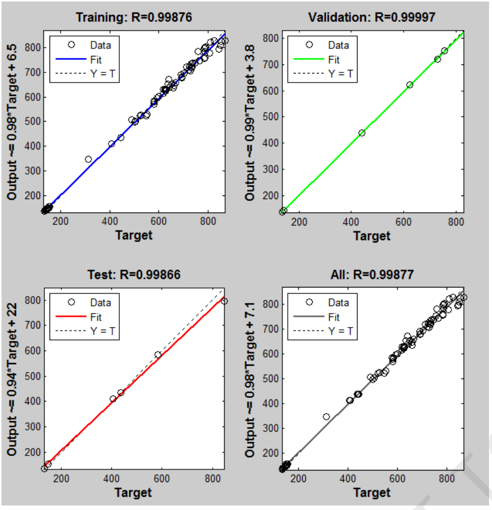


Figure 4 regression plots of the prediction network model

## 4. Result and analysis

With mapping relation between mirror target characters and mirror structure parameters from this prediction model, we can optimize mirror structure parameters for better mirror target characters. In order to drawing the relation between mirror target characters and mirror structure parameters directly, we assign a constant for two variables. Fig.5 shows mapping relation between output target characters and input structure parameters $x_1$,$x_2$(when $x_3$=$x_4$=6mm).

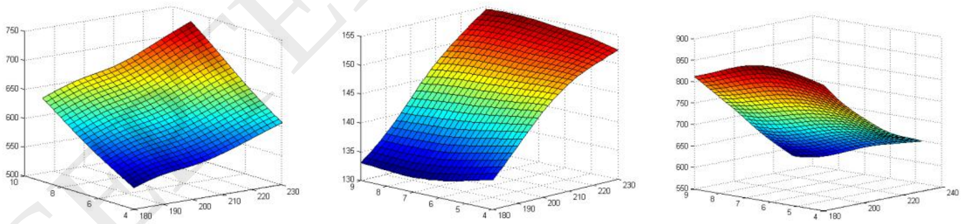

Figure 5 Mapping relation between outputs $M$, $f_1$, $RMS$ and inputs $x_1$,$x_2$ （$x_3$=$x_4$=6mm）

As can be seen from the left picture in Fig.5, with the increase of monolithic central thickness and face sheet thickness, mirror weight grows gradually. From the middle picture in Fig.4 we can see, when the monolithic central thickness is different, effect on first order constraint mode from face sheet thickness is different. When the monolithic central thickness is greater than 200mm, first order constraint mode increased with face sheet thickness. When the monolithic central thickness is less than 200mm, first order constraint mode is non-monotonic with influence of face sheet thickness. That is when face sheet thickness is greater than 7mm, first order constraint mode increased with face sheet thickness, when face sheet thickness is less than 7mm, first order constraint mode decrease with the increase of face sheet thickness. We can see that from the right picture in Fig.4, RMS present saddle-shaped face. In general, RMS decreases with the increase of monolithic central thickness. Fig.6 shows mapping relation between mirror output target characters and input structure parameters $x_2$,$x_3$(when $x_1$=200mm, $x_4$=6mm).

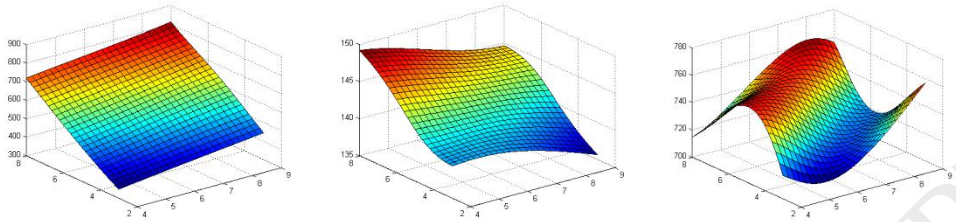

Figure 6 Mapping relation between outputs $M$, $f_1$, $RMS$ and inputs $x_2$,$x_3$ （$x_1$=200mm, $x_4$=6mm）

The above analysis shows that, the relation between mirror target characters and mirror structure parameters is too complex to describe by simple formula. With the nonlinear relation from neural network prediction model, we can seek optimal combination of structure parameters on certain demand. For the space-based large mirror, the surface shape error RMS under axial gravity reflects the stiffness of mirror, weight of mirror influence emission cost and the first order constraint mode will influence response of forced vibration and emission. The first order constraint mode of this mirror exceeds 130Hz, so the response of forced vibration and emission will be in the scope of control. In this issue, we define an optimization variable combination of weight and RMS as $OPT=0.7M+0.3RMS$ to find minimum. When $OPT$ is minimum, we regard the corresponding input mirror structure parameters as optimal parameters combination. Using Matlab programme, we attain the optimal combination of structure parameters through neural network prediction model. Prediction values and numerical simulation results of the optimal combination are shown in Tab.5 respectively. The prediction value's relative error are less than or equal to 6.69%.

Table 5 Result of parameter optimization

| Optimal combination | | | | $M(Kg)$ | | | $f_1(Hz)$ | | | $RMS(nm)$ | | |
|---|---|---|---|---|---|---|---|---|---|---|---|---|
| $x_1$ (mm) | $x_2$ (mm) | $x_3$ (mm) | $x_4$ (mm) | NN Prediction | FEA | Relative error% | NN Prediction | FEA | Relative error% | NN Prediction | FEA | Relative error% |
| 220 | 4 | 3 | 6 | 389.94 | 365.49 | 6.69 | 152.84 | 148.74 | 2.75 | 592.25 | 616.47 | 3.93 |

## 5. Conclusion

Output characters prediction model of space-based large mirror was built based on BP neural network. Training sample of neural network was obtained by taking advantage of orthogonal test design and numerical simulation. Orthogonal test design greatly decreases the test sample and guarantee that the test data is reasonable. As seen from the network extrapolation, the prediction relative errors of weight and first order constraint mode are less than or equal to 3.83%, the prediction relative errors of the mirror surface figure RMS error is less than or equal to 7.09%. Thus, this neural network prediction model with high precision extrapolation provides an ideal model for optimization of mirror structure. Taking advantage of this network model, we accomplish multi-parameter optimization of mirror output characters. The method can be used for solving other optimization problems refer to multi-parameter.

**Acknowledgements**

This research has been supported by Special Industrial Innovation Fund of JiLin Province((Grants No. 2018C040-1).

**References**

[1] Hagyong Kihm, Il Kweon Moon, Ho-Soon Yang, YunWoo Lee, 1-m lightweight mirror design using genetic algorithm, Proc. SPIE 841514(2012)
[2] Shutian Liu, Rui Hu, Quhao Li, Ping Zhou, Zhigang Dong, Renke Kang, Topology optimization-based lightweight primary mirror design of a large-aperture space telescope, Appl. Opt. 53,8318-8325 (2014)
[3] Yu-Feng Zhou, Yu-min Zhang, Jie-cai Han, Yuan-yuan Han, Wang Yao, Design and fabrication of large-scale RB-SiC mirror, Proc. SPIE 67210S(2007)
[4] Peng Guo, Jingxu Zhang, Fei Yang, Yan Zhang, "The design and analysis of 2m telescope's K Mirror system," Proc. SPIE 92800C(2014)
[5]Ke-rong Gai, "Study on large aperture SiC mirror technology," Proc. SPIE 84151G(2012)
[6] Hans J. Kaercher, "The mechatronic approach to the design of large mirrors and telescopes," Proc. SPIE 614802(2006)
[7] Xiao Yu, Fuzzy infrared image segmentation based on multilayer immune clustering neural network, Optik,140 (2017) 959-963
[8] Dawei Wang, Shuqing Zhang, Fanjiao Tan, Xiyang Zhi, Yongqiang Chu, Hongdi Lv, Rongkai Zhen, "A method on lightweight for the primary mirror of large space-based telescope based on neural network," Proc. SPIE 92981J(2014)
[9] Jing Zhang, YingPing Yang, JinMin Zhang, A MEC-BP-Adaboost neural network-based color correction algorithm for color image acquisition equipments, Optik, 127 (2016) 776-780
[10] Qiuhong Xiang, Bolin Liao, Lin Xiao, Long Jin, A noise-tolerant Z-type neural network for time-dependent pseudoinverse matrices, Optik, 165 (2018) 16-28
[11] Ruipeng Guo, Zhengsu Tao, A study of neural network for surface characteristics in-process optical measurement, Optik, 124 (2013) 2821-2824
[12] Anicet K. Kouakou, Olivier K. Bagui, Thérèse Atcham Agneroh, Adama P. Soro, Jérémie T. Zoueu, Cucumber mosaic virus detection by artificial neural network using multispectral and multimodal imagery, Optik, (2016) 11250-11257

[13] Bing Wu, Shaojun Han, Jin Xiao, Xiaoguang Hu, Jianxin Fan, Error compensation based on BP neural network for airborne laser ranging, Optik, 127(2016) 4083-4088
[14] Ashutosh Bagchi, S. Saravanan, G. Shanthos Kumar, G. Murugan, K. Raghukandan, Numerical simulation and optimization in pulsed Nd: YAG laser welding of Hastelloy C-276 through Taguchi method and artificial neural network, Optik, 146 (2017) 80-89
[15] Qitai Huang, Qiang Gao, Jingchi Yu, FEM analysis of ultra thin mirror supporting structure effect on surface deformation in gravity field, Proc. SPIE 61480W(2006)